Chem Soc Rev

ROYAL SOCIETY OF CHEMISTRY

TUTORIAL REVIEW

View Article Online
View Journal | View Issue

Cite this: *Chem. Soc. Rev.*, 2022, **51**, 7715

Medicinal inorganic chemistry – challenges, opportunities and guidelines to develop the next generation of radioactive, photoactivated and active site inhibiting metal-based medicines†

Raphael Lengacher, Axia Marlin, Dariusz Śmiłowicz and Eszter Boros *

Received 22nd May 2022

DOI: 10.1039/d2cs00407k

rsc.li/chem-soc-rev

Medicinal inorganic chemistry is a burgeoning subfield of medicinal chemistry that focuses on the development of metal-based diagnostic and therapeutic agents. This tutorial review aims to provide an introductory primer, present a timely overview of recent discoveries and identify current challenges and opportunities of the field. Three specific areas of discovery are highlighted herein. The first part focuses on metal-based radiopharmaceuticals for diagnostic and therapeutic purposes and specific design criteria for the development of radiopharmaceuticals that combine fundamental aqueous coordination chemistry with elucidation of pharmacokinetics. The second part describes approaches to photodynamic therapy with metal complexes. Here, photophysical characterization, combined with the challenge of careful control of the chemical behavior and selective biological deposition of transition metals with significant off-target toxicity, is discussed. In the third part, we summarize emerging strategies to modulate enzyme inhibition with coordination chemistry, while also highlighting the utility of the unique properties of metal ions for the characterization of mechanisms of action of these emerging diagnostic and therapeutic agents.

Key learning points

Metal complexes in nuclear medicine

• Radioisotopes are excellent tools for imaging by direct emission of imageable single γ photons (Single Photon Emission Computed Tomography) as well as photons that are produced by an annihilation event following a positron (β^+) decay (Positron Emission Tomography).

• Radiometals, which belong to beta (β^-), alpha (α) or Auger–Meitner emitters can be used as therapeutic radioisotopes, which deposit short-range, high-energy particles in target tissues.

Metal complexes and photodynamic therapy

• Metal complexes are well suited for the development of photodynamic therapeutics as their photophysical, and physicochemical properties can be readily tuned by modifying the metals' coordination sphere.

• Photodynamic therapy is subject to challenges due to the reliance on oxygen, the limited tissue penetration of light, and the inherent toxicity of heavy metals often used in PDT agents. Various strategies exist to alleviate these issues.

Metal complexes for enzyme inhibition

• Enzyme active sites can be efficiently targeted and inhibited by metal complexes by mimicking the substrate or binding and blocking of metallo-cofactors within metalloenzymes.

• Challenges remain for accurately predicting the interaction of coordination complexes with complex biomolecules and limiting off-target specificity; however, their intrinsic spectroscopic properties can help study their mechanism of action.

1. Introduction

Medicinal inorganic chemistry represents a subfield of medicinal chemistry, which uses exogenous metal ions as part of diagnostic agents and therapeutic drugs or small molecules that efficiently coordinate to endogenous, free metal ions and metal ions that constitute active parts of metalloenzyme active sites. Due to

Department of Chemistry, Stony Brook University, Stony Brook, 11790 New York, USA. E-mail: eszter.boros@stonybrook.edu

† Electronic supplementary information (ESI) available. See DOI: https://doi.org/10.1039/d2cs00407k

significant divergence of the spectroscopic, electrochemical and chemical bonding properties of metal ions, different challenges and opportunities arise for such systems, opening possibilities for drug development beyond those presented by scaffolds constructed from more commonly employed main group elements. However, involvement of metal ions in drug development also produces challenges that are unique to those elements due to their bioavailability, inherent toxicity and possible off-target behavior. This tutorial review will summarize select, recent developments of the medicinal inorganic chemistry field, focused on metal-based radiopharmaceuticals, metal complexes for photodynamic therapy of cancer and coordination complexes as inhibitors of enzyme active sites. While in no way exhaustive and complete, we aim to give a snapshot of recent, promising developments and outline gaps in knowledge that give rise to current opportunities within this rapidly growing field.

Raphael Lengacher

Dr Raphael Lengacher received his BSc and MSc degrees from the Swiss Federal Institute of Technology (ETHZ). Since then, he specialized in the field of organometallic- and radiochemistry. He obtained his PhD from the University of Zurich in 2021, where he worked in the group of Prof. Roger Alberto on the development of cyclopentadiene based Re/^{99m}Tc cancer theranostics. In November 2021, he joined the group of Prof. Eszter Boros, to investigate theranostic lanthanide complexes that can be excited by Cerenkov radiation.

Axia Marlin

Dr Axia Marlin received her BSc degree from University of La Reunion and MSc degree from University of Toulouse in France. Following her interest in Medicinal Inorganic chemistry, she joined the lab of Prof. Raphael Tripier where she worked on the synthesis and functionalization of tacn-based ligands as metal chelators for diagnostic and therapeutic applications. After obtaining her PhD in December 2021, she joined the group of Prof. Eszter Boros as a postdoctoral fellow in March 2022, where she develops synthetic, radiochemical and biological approaches to investigate new siderophore-based antibiotics for the treatment of bacterial infections.

Dariusz Śmiłowicz

Dr Dariusz Śmiłowicz obtained his BSc and his MSc at the Nicolaus Copernicus University (Poland). In 2020, he received his PhD in Chemistry from the Ruhr-Universität Bochum (Germany) in the group of Prof. Nils Metzler-Nolte, where he developed therapeutically relevant metal–peptide bioconjugates using Solid Phase Peptide Synthesis protocols (SPPS). Additionally, he was involved in the development of drug delivery systems selectively activated by cold plasma. Since November 2020, he is a postdoctoral fellow in the lab of Prof. Eszter Boros in the Department of Chemistry, Stony Brook University, where he develops new metal-based imaging probes and therapeutics for targeted anti-cancer therapy and approaches to the rapid synthesis of radiopharmaceuticals.

Eszter Boros

Dr Eszter Boros is an Assistant Professor of Chemistry with courtesy appointments in Radiology and Pharmacology at Stony Brook Medicine. Eszter obtained her MSc (2007) at the University of Zurich, Switzerland and her PhD (2011) in Chemistry from the University of British Columbia, Canada. She was a Postdoc (2011–2015) and later instructor (2015–2017) in Radiology at Massachusetts General Hospital and Harvard Medical School. In 2017, Eszter was appointed as Assistant Professor of Chemistry at Stony Brook University, where her research group develops new approaches to metal-based diagnostics and therapeutics at the interfaces of Radiochemistry, Inorganic Chemistry and Medicine. Her lab's work has been extensively recognized; Eszter has been named a 2020 Moore Inventor Fellow, the 2020 Jonathan L. Sessler Fellow (American Chemical Society, Inorganic Division), a 2021 ACS Infectious Diseases/ACS Division of Biological Chemistry Young Investigator (American Chemical Society), and a 2022 Alfred P. Sloan Research Fellow in Chemistry.

2. Radiometals in diagnostic and therapeutic nuclear medicine

2.1 Metal-based radiopharmaceuticals: a brief primer

Radioactive metal ions with suitable emission properties for nuclear medicine applications have long been part of medical physics, nuclear physics and nuclear chemistry basic research. With the emergence and broad accessibility of small, biomedical cyclotrons and portable generator systems to produce radioactive isotopes, perception of radioactive metal ions has shifted from basic research curiosities to viable, clinical tools for diagnostic and therapeutic nuclear medicine. The primary goal of imaging is to visualize the desired tissue and/or to localize potential disease, whereas the goal of therapy is to treat the disease, which was previously diagnosed and localized with the complementary diagnostic imaging method. Imaging requires the use of radionuclides that emit photons, either by direct emission of imageable single γ photons (Single Photon Emission Computed Tomography) or photons that are produced by an annihilation event following a positron (β^+) decay. Therapeutic radioisotopes are typically classified as beta (β^-), alpha (α) or Auger–Meitner emitters, which deposit short-range, high-energy particles in target tissues.[1] Due to the vast clinical success of ^{18}F-fluorodeoxyglucose, radiochemists have focused on method development centered on the formation of stable F–X bonds. Development of radiofluorination chemistry has enabled the synthesis of novel diagnostic radiopharmaceuticals but has not led to advances in therapeutic nuclear medicine. The reason for this is the lack of a suitable radioactive isotope of fluorine or a chemically similar element with therapeutic properties. However, numerous radioactive metal ions can be produced on a clinical scale with suitability for radiotherapy. In concert with a diagnostic radioisotope of the same element, or an element with similar chemical properties, it is possible to conduct sequential diagnostic and therapeutic intervention, commonly referred to as the theranostic approach (Fig. 1).

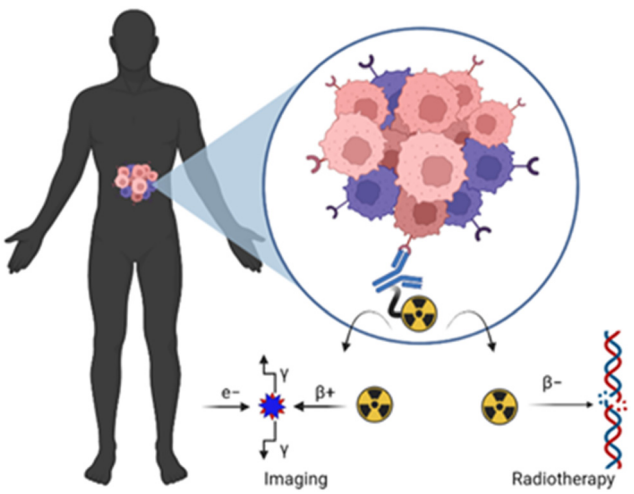

Fig. 1 Schematic description of the targeted theranostic approach using radiopharmaceuticals.

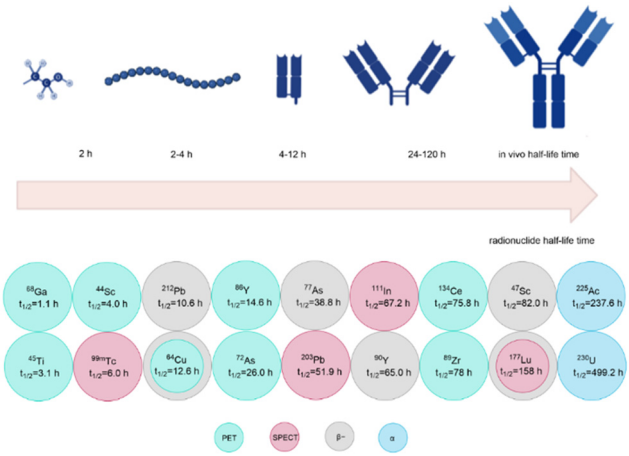

Fig. 2 Summary of metallic and metalloid radionuclides, their emissive properties, and half-lives, matched with the pharmacokinetic half-life of common biological targeting vectors.

In addition to consideration of emission properties, it is also important to match the isotope's half-life with the *in vivo* half-life of potential targeting vectors. Fig. 2 shows a summary of established and emerging radioactive isotopes of interest—many of which are metals or metalloids.

Ideally, the employed radionuclides form a matched pair—radioisotopes of the same chemical element—enabling use of an imaging radionuclide (*e.g.*, ^{64}Cu) to identify the sites of disease and subsequently a therapeutic radionuclide (*e.g.*, ^{67}Cu) to treat the disease. As only few elements have isotopes with suitable emission properties for this purpose, clinical applications have focused on perceived chemical homologues. Besides 16 approved, ^{99m}Tc-based radiopharmaceuticals that were established after the first emergence of ^{99}Mo/^{99m}Tc generator and chemistry to transform $^{99m}TcO_4^-$ into various other chemical forms, other radiometal-based radiopharmaceuticals have recently gained approval by the Food and Drug Administration (FDA). We defer to comprehensive and informative review articles by others which extensively explored the Tc-chemistry over 3 decades.[2]

To date, the FDA has approved the following metal-based radiopharmaceutical for therapy beyond ^{99m}Tc: ^{223}Ra for treating bone metastases arising from prostate cancers; ^{177}Lu-labeled DOTA-TATE for treating somatostatin receptor positive gastroenteropancreatic neuroendocrine tumors as well as ^{177}Lu-PSMA-617, a targeted radiotherapy agent to treat neuroendocrine carcinomas. For diagnostic purposes, ^{64}Cu-DOTA-TATE was approved for localization of somatostatin receptor positive neuroendocrine tumors in adult patients; ^{68}Ga-PSMA-11 (PET) as well as a $^{99m}Tc(CO)_3$-PSMA SPECT agent have emerged as diagnostic agents for PSMA-positive prostate cancer, ^{68}Ga-DOTA-TATE for imaging somatostatin-receptor-positive neuroendocrine tumors (Fig. 3). Evidently, as access to radiometals continues to improve, diversification of strategies to transform these isotopes into radiopharmaceuticals are needed and represent a highly active field of research. In this section, we introduce essential design strategies for metal-based

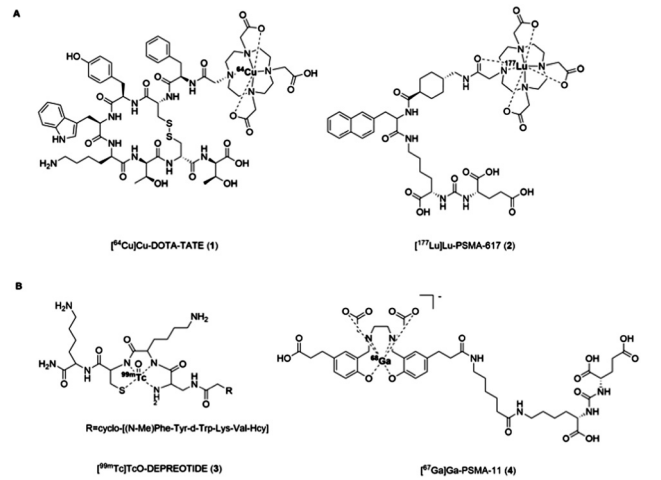

Fig. 3 Examples of metal-based radiopharmaceutical for (A) radiotherapy and (B) diagnostic imaging.

radiopharmaceuticals and highlight current challenges and opportunities for development.

2.2 Chelation strategies for radiometals: design criteria

To achieve targeted delivery of radioactive isotopes, bifunctional chelates require chemical linkage of a targeting vector. These constructs must fulfill specific criteria that relate to (a) the on-kinetics of the metal binding event, (b) the off-kinetics of the metal binding event, as well as (c) the binding of the entire construct to the target *in vivo*. Fig. 4 summarizes requirements relating to different components of the bifunctional chelate, which inform the following design criteria:

(1) Prior to incorporation of the radiometal, the entire construct must be assembled and be stable under conditions commonly used for radiometal chelation. As the half-life of radioactive isotopes can be as short as only a few minutes, radiolabeling should be conducted as the last step prior to purification, sterile filtration and dose preparation for administration. Therefore, constructs ought to be stable and soluble in aqueous media between pH 4–9 for extended time periods.

(2) Radiochelation should ideally occur under mild conditions within a short reaction time resulting in a high radiochemical yield.

(3) For radiolabeling conditions incompatible with biomolecules, once the radiometal chelate is formed, it must undergo facile conjugation to desired targeting vectors simultaneously retaining the original target affinity of the conjugated vector, as described by the K_d value.

(4) Following *in vivo* administration and circulation, the conjugate should exhibit high kinetic inertness to avoid the loss of the metal ion.

These design criteria have been fulfilled for clinically employed radiopharmaceuticals, mostly as appropriate bifunctional chelators have been established and tested for their biocompatibility. However, many emerging radiometals with attractive properties for imaging and therapy do not have established chelation approaches. Below, we highlight several representative metal ions with radioactive isotopes of interest where novel chelation strategies have recently been reported.

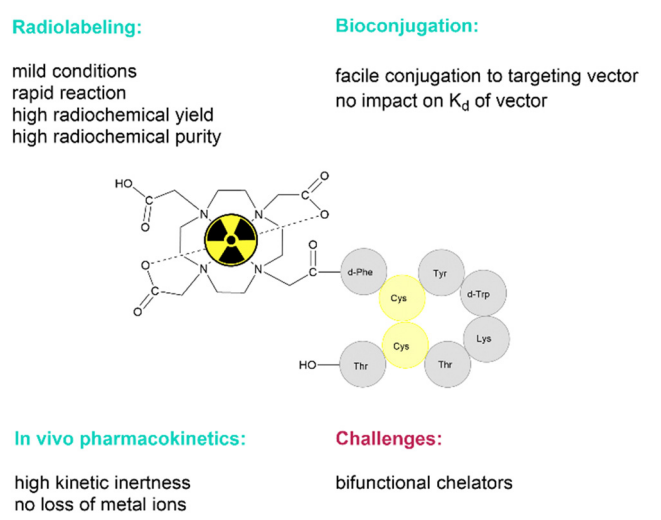

Fig. 4 Design criteria for bifunctional chelators for radioisotopes.

2.3 Current challenges and opportunities

2.3.1 Chelation of lanthanide/actinide alpha emitters of interest: Ac, Th^{4+}, $Ce^{3+/4+}$ and $U^{4+/5+/6+}$. The past decade has seen growing interest in the production of promising α-emitting isotopes such as ^{225}Ac and ^{227}Th for radiotherapy. Early clinical trials with these isotopes indicate that they have high potential for the treatment of late-stage cancers, especially when radiotherapy with β^- emitting isotopes, such as ^{177}Lu, fails. However, numerous shortcomings exist arising from the lack of stable chelation strategies to incorporate these isotopes into radiopharmaceuticals.[3]

The ^{225}Ac isotope ($t_{1/2}$ = 9.9 days, E_{max} = 5.83 MeV, α) emits four α particles and has produced promising results in treating β^- therapy resistant prostate cancer in clinical trials using a peptide-based targeting vector. Antibodies, albeit powerful targeting moieties, remain underexplored with actinium-225 due to a lack of compatible radiochemical labeling approaches that do not jeopardize the biomolecule's integrity. One of the main challenges in developing suitable chelators for $^{225}Ac^{3+}$ is the metal's weak electrostatic interactions with ligand donor atoms caused by its low charge density. Research on the subject has been mostly restricted to limited series of chelators, namely DOTA (1,4,7,10-tetraazacyclododecane-1,4,7,10-tetraacetic acid), HOPO (hydroxypyridinonate) and macropa (*N*,*N*′-bis[(6-carboxy-2-pyridyl)methyl]-4,13-diaza-18-crown-6) chelators (Fig. 5). The latter two differ significantly in their selectivity for large 3+ and 4+ cations. HOPO chelators exhibit exceptionally high stability with tetravalent ions including Zr^{4+}, Th^{4+} and Cr^{4+} (*vide infra*), while macropa is better suited to chelate trivalent and bivalent large cations including La^{3+}, Ac^{3+}, Ba^{2+} and Ra^{2+}.

The balance between chelator selectivity *versus* promiscuity is difficult to strike, as both approaches suffer from significant challenges. Highly ion-selective chelators are often difficult to

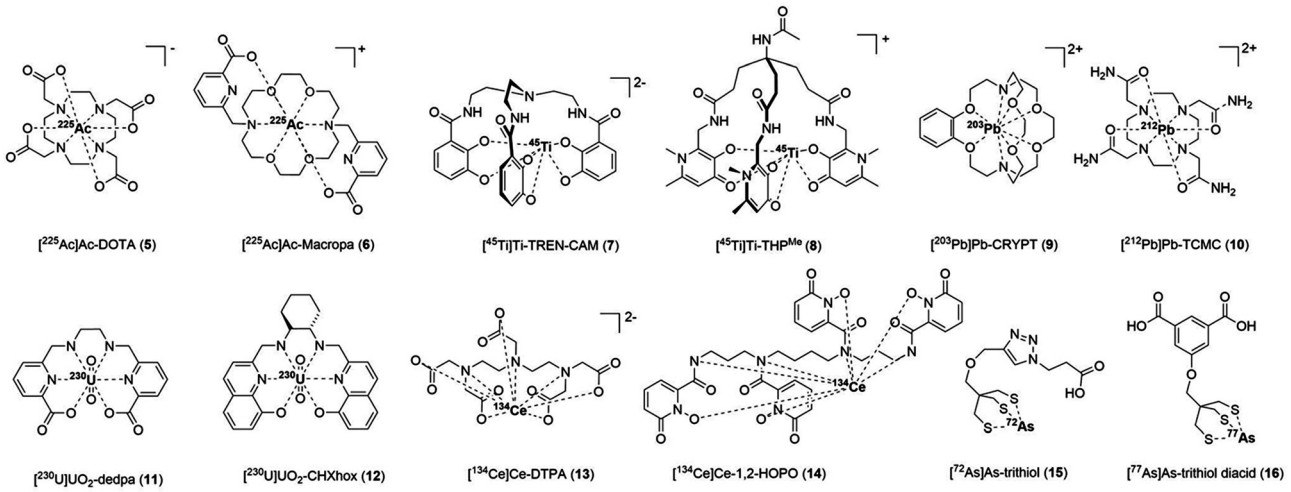

Fig. 5 Examples of stable chelation systems for emerging radioisotopes.

develop using a straightforward approach, especially for ions with underexplored coordination chemistry such as the late f-elements. Promiscuous chelators may offer labeling with different isotopes of interest for nuclear medicine, but might produce coordination complexes of limited kinetic inertness, thus the two strategies must be weighed carefully for any isotope of developmental interest. Another exemplary case for this is chelator development undertaken for the α-emitting radionuclide, uranium-230 ($t_{1/2}$ = 20.8 d, E_{max} = 5.8 MeV, α). The anionic oxygen-donor, acyclic hexadentate oxine-derived chelating ligands H_2dedpa, H_2CHXdedpa, H_2hox, and H_2CHXhox, have been identified as promising chelators based on the chemically hard and oxophilic nature of the UO_2^{2+} ions, the most stable species of uranium in aqueous solution (Fig. 5). The corresponding ^{230}U complexes showed high stability supported by reduced bone uptake in comparison to free uranium-230 salt. Evidently, while UO_2^{2+} coordination chemistry in anhydrous solvents has been subject to long-standing interest in the f-element community, stabilization of chelation in biological media is to date widely lacking yet an attractive emerging challenge with importance for nuclear medicine applications.[4]

Another significant challenge for the development of f-elements as radiopharmaceuticals is the lack of available diagnostic congeners. Small ions with PET isotopes, such as Sc^{3+}, Y^{3+} and Zr^{4+} cannot accurately capture the chemical behavior, and as a result, biological properties of the large tri- and tetravalent f-elements.[5] To this end, controlled modification of the oxidation state of cerium using ^{134}Ce ($t_{1/2}$ = 75.8 h, Auger L3-X = 46%, E_{max} = 5.3 keV) has been proposed as a versatile imaging partner for either $^{225}Ac^{3+}$ or $^{227}Th^{4+}$. As the redox states 3+ and 4+ are both accessible for Ce in aqueous media, chelators can be selected to stabilize the desired redox state. As such, ^{134}Ce was stabilized in oxidation state 3+ with diethylenetriamine pentaacetic acid (DTPA) ligand to use $^{134}Ce^{3+}$ as a PET isotope to predict therapy with $^{225}Ac^{3+}$, whereas chelation by an octadentate chelator, HOPO, changes the ^{134}Ce oxidation state to 4+ enabling direct homology with $^{227}Th^{4+}$ (Fig. 5).[6]

2.3.2 Capturing exceptionally hard ions with underexplored aqueous chemistry: V^{5+} and Ti^{4+}. The radionuclide ^{45}Ti ($t_{1/2}$ = 3.08 h, β^+ = 85%, E_{β^+} = 439 keV, E_{β^+max} = 1.04 MeV) has emerged as a promising isotope for positron emission tomography (PET) imaging due to its high positron branching ratio (85%), low emission of concurrent gamma (<1%) and low average positron energy (439 keV), making its imaging quality comparable to the widely clinically used PET isotope ^{18}F ($t_{1/2}$ = 109.8 min, β^+ = 96%, E_{β^+avg} = 250 keV). Additionally, a half-life of 3.08 hours is ideal for combination with targeting vectors that exhibit short pharmacokinetic half-lives.[7] However, the poor stability of most Ti^{4+} species in aqueous environments has hindered development of the titanium-45 isotope for PET imaging applications. Various titanium complexes have been prepared as titanocene dichloride, budotitane, and *N*,*N*′-bis-(salicylidene)ethylenediamine (salen) complexes. Unfortunately, they exhibit poor *in vivo* stability as the consequence of hydrolysis of the Ti^{4+} ion, resulting in significant decomplexation and transchelation in biological media. Moreover, the synthesis of such complexes requires organic solvents and high temperature conditions which is not compatible with the synthesis of biocompatible radiopharmaceuticals. As Ti^{4+} possesses a comparable ionic radius to Fe^{3+} (Fe^{3+} = 0.645 Å, Ti^{4+} = 0.605 Å) as well as a preference for 6-coordinate octahedral geometry, Ti^{4+} complexes with hexadentate analogues of catechol (benzene-1,2-diol), deferiprone (3-hydroxy-1,2-dimethyl-4(1*H*)-pyridone) and *N*,*N*′,*N*″-(nitrilotris(ethane-2,1-diyl))tris(2,3-dihydroxybenzamide) (TREN-CAM), have recently been reported as potential solutions to this problem (Fig. 5). Both chelators formed stable ^{45}Ti complexes across a wide pH range and demonstrated considerable *in vivo* compatibility.[8]

Vanadium-48 ($t_{1/2}$ = 15.97 days, β^+ = 49.9%, E_{β^+avg} = 290 keV), a positron emitting radionuclide, is another emerging isotope of a hard ion that has received considerable attention for the study of slow metabolic processes due to its relatively long

half-life. To date, only simple complexes such as ^{48}V labeled vanadyl (VO^{2+}) bis(acetylacetonato)oxovanadium(IV) [$VO(acac)_2$] have been prepared and evaluated *in vivo*.[9] The imaging application of ^{48}V remains in its infancy due to the lack of stable chelation approaches. As a consequence, ^{48}V, together with ^{45}Ti are isotopes with considerable potential for development with respect to even their fundamental separation and chelation chemistry.

2.3.3 Capturing exceptionally soft ions and metalloids with underexplored aqueous chemistry. Arsenic-72 and arsenic-77 represent a ''true matched pair'' with identical chemical properties and thus the same *in vivo* biological behavior. Arsenic-72 ($t_{1/2}$ = 26 h, β^+ = 64%, $E_{\beta^+\max}$ = 2.49 MeV, $E_{\beta^+\max}$ = 3.33 MeV, β^+ = 16%, γ = 81%, $E_{\max}$ = 834 keV) and ^{77}As ($t_{1/2}$ = 38.8 h, $\beta^-_{\max}$ = 97%, $E_{\max}$ = 0.683 MeV, γ = 1.59%, E_γ = 239 keV) are radioisotopes potentially useful for PET and radiotherapy, respectively. Since the thiophilic nature of arsenic is well-established, several thiol ligands for radioarsenic complexation have been tested. Specifically, dithiolates such as dimercaprol, 2,3-mercaptosuccinic acid (DMSA) and aryl–trithiol ligands (Fig. 5). However, such complexes are often hydrophobic resulting in significant hepatobiliary clearance, likely in part due to As-dissociation. One of the key challenges of radioarsenic chemistry are the need for concomitant reduction of As^{5+} upon coordination to coordinatively stabilized As^{3+}; while this is feasible with thiols, the subsequent tendency for dissociation and back-oxidation to As^{5+} remains a challenge. Recently, a bifunctional trithiol chelator with high *in vitro* stability and improved hydrophilicity has been reported, but targeted imaging and therapy studies have not been reported at this time. Clearly, the coordination of an unusual metalloid such as As to afford a biocompatible and inert chelation complex with the As^{3+} or As^{5+} core, remains an active area of research.[10,11] Another comparatively soft, yet non-redox active metal ion of interest for nuclear medicine applications is Pb^{2+}. Specifically, lead-212 (^{212}Pb, $t_{1/2}$ = 10.6 h, β^- = 100%, $E_{\max}$ = 0.57 MeV) and lead-203 (^{203}Pb, $t_{1/2}$ = 51.9 h, γ = 81%, E_γ = 279 keV, SPECT) represent a matched theranostic radioisotope pair for application in targeted radionuclide therapy and single-photon emission computed tomography (SPECT), respectively.[12] Originally, the DOTA ligand was used for radiolabeling with ^{212}Pb resulting in kinetically stable Pb-DOTA complexes. However, the release of Pb *in vivo* in the acidic tumor environment was observed and as the consequence a more efficient and stable chelate, 1,4,7,10-tetra-(2-carbamoyl-methyl)-cyclododecane (TCMC) has been introduced for Pb labeling, and more recently, a bicyclic cryptand-like system, Pb-CRYPT (Fig. 5).[13] Such chelators provide excellent radiolabeling at room temperature as well as high *in vitro* stability. One of the challenges for the coordination of lead-212 with soft Lewis basic ligands is decay to the comparatively long-lived daughter nuclide $^{212}Bi^{3+}$. Bi^{3+} exhibits coordinative preferences more comparable to hard or borderline Lewis acids, resulting in a loss of affinity for chelators that are selective for Pb^{2+}.[14] Therefore, chelators that can stabilize both ions by conformational or coordinative toggling are of potential interest in this area.

2.4 Emerging topics of interest

For radiometal chemistry, a significant challenge remains the correlation of macroscopic coordination chemistry studies including stability and kinetics with reactivity under trace radiochemistry conditions. These differences lead to discrepancies in the observed on- and off-kinetics, further complicating the predictability of radiochemical behavior. Thermodynamic stability constants, acid-dissociation kinetics, and chelator-to-chelator challenge assays, while representing state of the art characterization tools, are not reliably predictive of the *in vitro* and *in vivo* behavior of corresponding radiochemical coordination complexes. Therefore, a holistic, critical approach to the development of radiopharmaceuticals taking into consideration similarities and differences between macroscopic, non-radioactive chemistry and microscopic, tracer radiochemistry remains desirable.

3. Metal complexes and photodynamic therapy

3.1 Introduction

Photodynamic therapy (PDT) is defined as the combination of a photosensitizer, light and the production of singlet oxygen which causes Fenton/Fenton-like chemistry. The resulting oxidative stress to the host cell results in apoptosis, that, if induced selectively for target tissues, results in a desirable therapeutic effect.

Most chemotherapeutic drugs exhibit non-specific off-target effects and resistance that can lead to life-threatening, systemic issues and minimize therapeutic efficacy. PDT circumvents this issue, as the spatial and temporal activity of the drug can be precisely controlled through its activation by light. Light can be administered selectively with respect to irradiation location and time. Organic photosensitizers for PDT are mainly based on the porphyrin, phthalocyanine, boron-dipyrromethene (BODIPY), and indocyanine green structures (Fig. 6). For example, Photofrin® (**17**), an FDA approved PDT agent, is composed of a mixture of porphyrin oligomers. However, control of the photophysical properties of organic photosensitizers, dominated by π to π* transitions, is restricted to expansion or contraction of

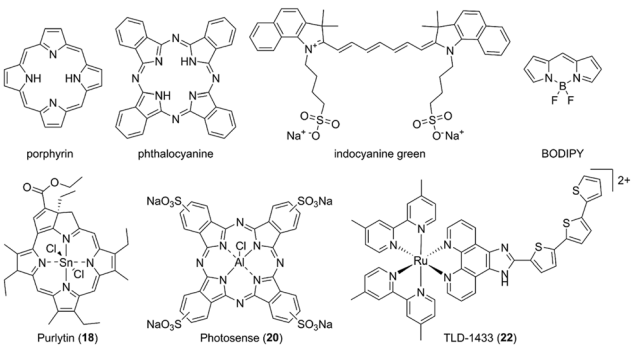

Fig. 6 Structures of clinically translated, organic PDT agents (top) and examples of metal-based PDT agents (bottom).

such aromatic π systems, as well as the incorporation of hydrophilic functional groups to enhance solubility in biocompatible solution media.

Transition and f-block metal complexes offer a convenient alternative, as their photophysical and physicochemical properties can be readily tuned by modifying the metal's coordination sphere. This flexibility arises from (1) access to a larger variety of excitation and de-excitation mechanisms of coordination complexes and (2) the chemical modularity of coordination complexes assembled from various ligand and metal ion building blocks. Exploiting these characteristics, various FDA approved PDT drugs have been developed to date, incorporating metals such as Sn (Purlytin® (**18**)), Lu (Lutrin®/Antrin® (**19**)), Al (Photosens® (**20**)), and Pd (TOOKAD® (**21**)) to the porphyrin and phthalocyanine structures (Fig. 6). Other *de novo* complexes have been developed and tested, primarily using metals Ru, Ir, Os, Re, and Pt. Most notably, Ru complex TLD-1433 (**22**), is the first Ru^{2+} based photosensitizer to undergo human clinical trials. Its main photoexcitation occurs between 300–550 nm, thereby, it can be excited by green light. The cytotoxicity has been demonstrated in four different cell lines (CT26-CL55, U87, F98 and CT26.WT); at concentrations between 0–180 μM all showed minimal dark toxicity and 100% cell death under light irradiation for concentrations as low as 1 μM (U87 and CT26.WT cell lines).[15] Following successful phase 1 and 2 clinical trials, TLD-1433 has recently been approved for phase 3 trials to treat advanced stage bladder cancers.

3.2 Design criteria for PDT agents

PDT agents are categorized according to their mechanism of action. In this review, we cover type I and type II PDT agents, as well as photoactivated chemotherapeutics (PACT).

Type I and type II PDT agents are excited by light from the singlet ground state (GS) S_0 to an excited singlet state S_1 (Fig. 7). By undergoing intersystem crossing to the triplet state T_1, possible transfers to ligand-based excited states can occur. From the metal centered triplet state T_1, type I and type II mechanisms diverge but consistently produce singlet oxygen. Singlet oxygen production is the primary pathway to induce apoptosis without further transformation or degradation of the coordination complex. Several other pathways can occur as well, not all of them leading to the generation of ROS. In the case of $[Ru(bpy)_2(dppn)]^{2+}$ (**23**), a ligand centered triplet state T_1L is accessed, which is lower in energy than the metal centered T_1M state. This offers a deexcitation pathway that does not produce ROS which is believed to directly oxidize guanine bases and thereby leading to DNA photocleavage (Fig. 8). In the case of complex $[Ru(bpy)_2(pyrene)]^{2+}$ (**24**), the ligand centered triplet state T_1L and the metal centered T_1M state are very close in energy, which allows rapid transition and access to both states (Fig. 8). As a result, two different deexcitation pathways are available. It has been hypothesized that the T_1L state is responsible for the generation of $^1O_2$, while the T_1M state can directly oxidize guanine nucleobases. By varying both the T_1M and the T_1L state energies, one pathway can be favored over the other. For example, in hypoxic tumors a pathway independent of molecular oxygen might lead to better results.

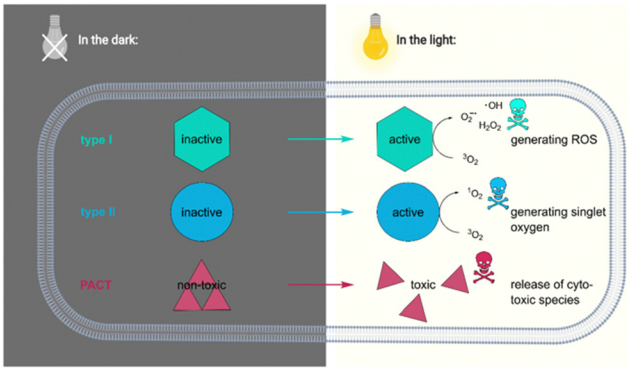

Fig. 7 General mode of action for type I and type II photodynamic therapy agents as well as photoactivated chemotherapeutics.

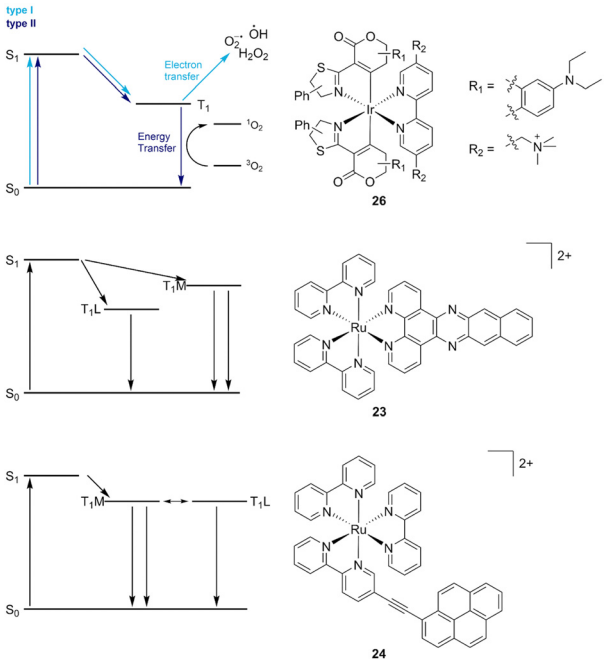

Fig. 8 Jablonski diagrams of different excitation and deexcitation pathways for different metal containing PDT agents.

In contrast, photoactivated chemotherapeutics undergo a chemical transformation that allows the release of one or more reactive species from the metal center, which can comprise released ligand or the activated metal-complex, to produce the desired chemotherapeutic effect. Examples are the release of CO as seen in photoCORMs or the reduction of octahedral Pt^{4+} prodrugs to square planar Pt^{2+} compounds.

Coordination complexes that serve as effective PDT agents are composed of a metal ion with slow on- and off-kinetics, coordinated by ligands that produce accessible, long-lived, and reactive excited states. Slow kinetics are required for complexes where the coordination environment is to be preserved to prevent degradation and accumulation in healthy tissues.

Therefore, second and third row transition metals are better suited for PDT agents of type I and type II.

On the other hand, photoactivated chemotherapeutics require rapid transchelation or ligand release kinetics once the activation occurs. As a result, first row transition metal complexes are better suited for this type of mechanism and/or kinetically more labile electronic configurations of second and third row transition metal complexes.

For both types of mechanisms, compounds should ideally have high kinetic inertness in their inactive state and exhibit a large difference in dark *versus* light toxicity, expressed by the photodynamic index (PI). Kinetic inertness of the metal complexes is of particular importance, as the photosensitizer should stay intact *in vivo*. If both metal and ligands are released in reactive forms, off-target toxicity may occur. As most inorganic/organometallic photosensitizers (PSs) are composed of heavy metals, many can bind to the active site of metalloproteins and act as potent ''catalyst poisons''. To avoid off-target toxicity, a large difference between light and dark toxicity is vital. Specifically, light toxicity should be accessible at concentrations where dark toxicity is negligible, but delivery to target tissues *via* systemic administration is still feasible. This is especially important for most PDT agents that have no inherent targeting ability to the tissues of interest. For instance, the organic PS **25** has a PI of 88.33, meaning that it is more than 88 times more effective in irradiated tissue than in the dark. As no EC_{50} has been determined for **26**, no definite PI value can be determined. However, it is at least 540 times more effective under light irradiation. A list of representative PDT agents and their corresponding PIs can be found in Fig. 9 and Table 1.

In addition to a large photodynamic index, access to excited states should be efficient and rapid. Therefore, potential PDT agents require high quantum yields to enable the generation of $^1O_2$ (type II) or other ROS (type I). Furthermore, the triplet state of the PS should be long lived, to provide sufficient time for the excited PS to diffuse to $^3O_2$ prior to relaxation to the ground state. These lifetimes should be within the microsecond range. Additionally, pharmacokinetic factors need to be addressed: PSs need to be water soluble and stable in biological media, reach target tissue and, if possible, should accumulate therein to produce increased therapeutic effects and decrease off-target toxicity.

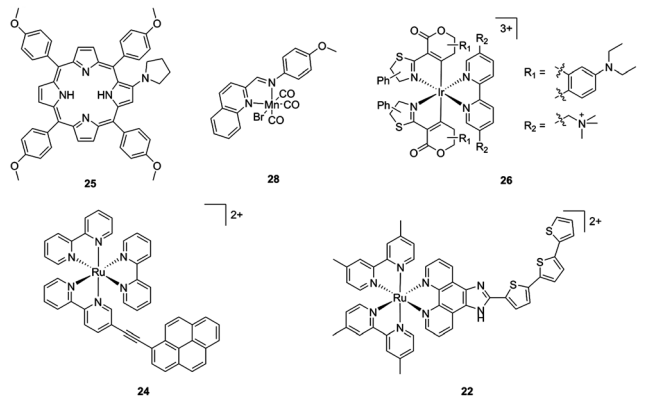

Fig. 9 Structures of compounds discussed in Table 1.

Table 1 Selected photodynamic therapy agents with their dark toxicity, light toxicity, photodynamic index (PI), and the cell line they were investigated in

Compound	Dark toxicity EC_{50} [μM]	Light toxicity EC_{50} [μM]	PI	Cell line
25	386.9	4.38	88.33	HeLa[16]
28	50	7.1	7.04	HeLa[17]
26	>200	0.37	>540	HepG2-SR[18]
24	262	0.15	1747	HL60[19]
22	137	0.00019	721 000	SK-MEL-28[20]

3.3 PDT agents that generate singlet oxygen

For PDT agents of type I, the excited triplet state generates ROS such as hydroxyl and superoxide radicals *via* electron or hydrogen transfer from the excited state. In the type II mechanism, an energy transfer from the excited triplet state to molecular triplet state oxygen ($^3O_2$) occurs, forming highly reactive singlet oxygen ($^1O_2$). These two mechanisms are, however, not mutually exclusive, which is exemplified in iridium complex **26**, which is able to undergo both mechanisms. **26** exhibits high phototoxicity with IC_{50} values of 1.6 μM (A549R cisplatin resistant cell line) and 0.37 μM (HepG2-SR sorafenib resistant cell line) with no observable dark toxicity at concentrations of up to 200 μM.[18]

Currently, this field explores photosensitizers that absorb in the visible range, especially in the red or NIR region (600–900 nm), as light at those wavelengths has increased tissue penetration. As this might be true for classical PDT with external light sources, it might not be the case if internal or *in situ* photon sources can be co-delivered with the PDT agent. For instance, if a PS uses Cherenkov radiation (CR) a red shifted absorption is counterproductive, as CR intensity is the highest in the UV and blue range. Therefore, the ideal absorption range of a PS should be in accordance with the wavelength of the intended photon source.

3.4 Photoactivated chemotherapeutics

Light can be used in different ways to activate prodrugs and transform them into their active species without reliance on molecular oxygen. Photoactivated chemotherapeutics are activated by the release of a cytotoxic compound from the inert photosensitizer. For instance, organometallic carbonyl complexes can release CO upon photoexcitation, termed photo-CO-releasing molecules (photoCORMs). An example is the Mn^+ complex **27**, which can be excited with blue light (479 nm) and releases CO as a result. Exchanging the pyridine ligand with a quinoline leads to a red shift of the absorption maxima to green light (512 nm) for complex **28**. Compound **28** has a phototoxicity of 7.1 μM (HeLa cell line) and no dark toxicity below 50 μM (Fig. 10, top).[17]

Another example for inactive metal containing prodrugs that can be photoactivated are Pt^{4+}–Pt^{2+} systems. Non-toxic Pt^{4+} compounds can be photoreduced to the active Pt^{2+} drug. This requires the redox potentials of the prodrug to be accessible

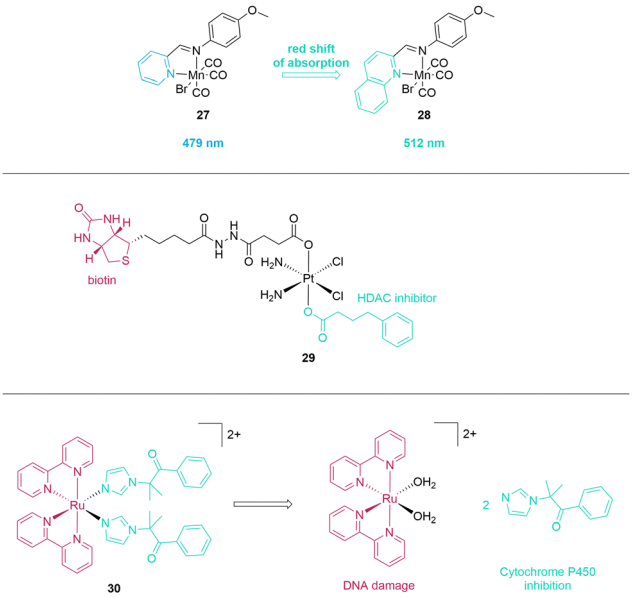

Fig. 10 Top: Design of photoCORM **28**, which can be excited by green light to release CO. Replacing the pyridine ligand (blue) with a quinoline ligand (green) leads to a red shift of the absorption maxima of roughly 30 nm, allowing the use of green light for excitation which expresses increased tissue penetration compared to blue light. Middle: Structure of **29**, a photoreducible Pt^{4+} prodrug bearing biotin, and a histone deacetylase inhibitor. Bottom: Light induced ligand dissociation in **30**, releasing three bioactive compounds.

under biological conditions. For instance, six-coordinate, octahedral Pt^{4+} complexes can effectively overcome the non-selective toxicity and acquired drug-resistance associated with Pt^{2+} drugs.

Pt^{4+} prodrugs can be accessed by oxidation, carboxylation and ligand substitution of Pt^{2+} precursors. Ligands in the axial position can be employed to tune the properties of the corresponding Pt^{4+} complexes or to append a targeting moiety.[21] The corresponding bifunctional Pt^{4+} prodrug complexes can subsequently be selectively photoreduced to release the active Pt^{2+} species. Octahedral, low spin d^6 Pt^{4+} complexes are more kinetically inert than their square planar Pt^{2+} counterparts, allowing fewer side reactions before the target site is reached and the complex is reduced selectively to its active, Pt^{2+} form under release of the axial ligands. The corresponding Pt^{4+} complexes contain spectator ligands within the equatorial plane, which remain part of the Pt^{2+}–DNA adduct following the dissociation of labile ligands such as halides to enable reaction with the purine bases of DNA. As such, photoreleasable pro-drugs as axial Pt^{4+} ligands provide multifunctional drug action. A recent example includes the conjugation of Pt^{4+} drug with histone deacetylase inhibitors (HDACi). Pt^{4+}Ac-POA includes 2-(2-propynyl)octanoate (POA) as HDAC inhibitor. The presence of POA enhances the DNA exposure to the active Pt^{2+} complex after the reduction mechanism in the tumor environment.[22] Complex **29** is another good example of a multifunctional Pt^{4+} prodrug by incorporation of 4-PBA and a targeting moiety with the biotin group (Fig. 10, middle). The complex is an efficient prodrug since its toxicity is much lower than that of cisplatin in human normal liver cells.[23]

Yet another way is the light induced dissociation of ligands, releasing one or more therapeutically active species from an inert (inactive) coordination complex. The study of the mechanism of action of such compounds is complicated by evaluation of all possible reactive species for their corresponding toxicity. An example are the Ru complexes developed by Zamora *et al.*, which release two of their ligands under light irradiation.[24] The released complex inflicts DNA damage to the host-cell, while released ligands can also act as inhibitors of cytochrome P450, an essential housekeeping enzyme involved in electron transfer. For example, **30** produced a PI of 136 for inhibition of P450 (Fig. 10, bottom).

3.5 Current challenges and opportunities

As with all possible approaches to treat a disease, photodynamic therapy is subject to various restrictions and challenges. This section outlines current challenges and discusses different approaches as to how these various challenges are currently being addressed.

3.5.1 Eliminating the reliance on oxygen. One limitation to PDT is the reliance on molecular oxygen for the generation of therapeutically active ROS. Due to their fast growth and insufficient blood supply, cancer cells are often hypoxic (oxygen deficient). This impedes the efficacy of many PDT agents. Additionally, PDT further depletes the cell of oxygen and damages blood vessels, which leads to further decreased blood flow and by limiting oxygenation (Fig. 11).

Various approaches exist to address this issue; a recent review covers them comprehensively.[25] One of the primary strategies is to oxygenate the targeted tumor tissue by codelivery of molecular oxygen with the PDT agent. This can be done by hemoglobin, perfluorocarbons, metal–organic frameworks (MOFs), or directly by the decomposition of solid peroxides at the target site. Another strategy explores increase of blood flow within the tumor by anti-angiogenic agents. Furthermore, cell respiration can be temporarily inhibited, thereby reducing O_2 consumption within the cell to increase reactive O_2 levels.

A different strategy is to eliminate the dependency on molecular oxygen at the target site by designing molecules that

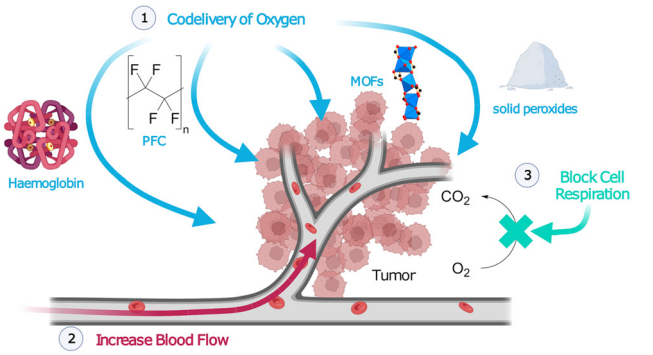

Fig. 11 Different strategies to increase the concentration of molecular oxygen in tumor tissue.

release cytotoxic species under light irradiation such as $^{\bullet}OH$, O_2^-, $^{\bullet}Cl$, NO, CO, H_2S, or SO_2. Even $^1O_2$ can be directly released by the selective and light-induced ring opening of endoperoxides. This, however, brings the distinct disadvantage that only one equivalent of cytotoxic species is generated per molecular PDT species.

3.5.2 Addressing the limited tissue penetration of light. While irradiation of the affected areas works well for localized, superficial disease, deep tumor therapy is restricted by the tissue penetration of light, which is wavelength dependent. Short wavelength light, including ultraviolet (UV) and blue light, has very limited tissue penetration but is typically most efficient to access to excited states of PDT metal complexes. PS **31** for instance is excited by blue light. With increasing wavelength, tissue penetration increases as well and reaches a maximum in the red and near infrared (NIR) spectrum (PS **28** gets excited by green and PS **32** gets excited by red light). This has been addressed in part by the extension of π systems of the ligands, as well as the shift to third row transition metals such as Os from Ru to access smaller energy gaps to long-lived excited states. However, in the absence of a targeting vector and full-body irradiation, this strategy still requires tumor localization prior to therapeutic intervention (Fig. 12).

One way to account for this limitation is to design PSs that can be activated at other wavelengths, such as red/NIR light or X-rays. The design of such PSs, however, is challenging and has its own limitations as the tissue penetration of NIR light is also limited. Additionally, the ionizing nature of X-rays might have undesired adverse side effects. To bypass these limitations, *in situ* generated, "internal" light sources have emerged as a potential solution (Fig. 13): chemiluminescence (CL), bioluminescence (BL), and Cherenkov radiation (CR).[26] Chemi- and bioluminescence arise from chemical/enzymatic reactions that produce light as a byproduct. CL is most commonly produced by reactions of oxalate esters or luminol with H_2O_2. A special case of CL is the production of luciferin catalyzed by the luciferase enzyme. Cherenkov radiation (CR) arises from charged particles that travel through a dielectric media such as water at speeds higher than the speed of light in that

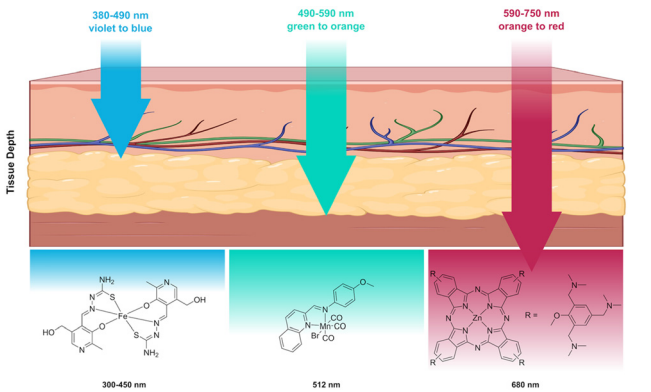

Fig. 12 Penetration depth of light in tissue depending on wavelength. For every window, a metal-based PDT agent is shown that can be excited with light of the corresponding wavelength.

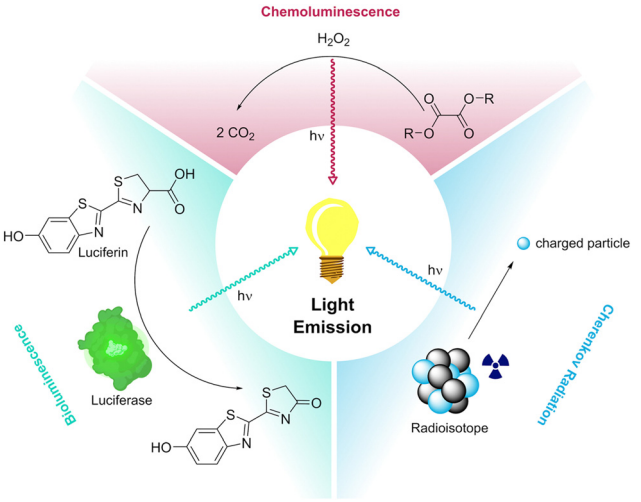

Fig. 13 Internal light sources employed for the activation of PDT agents without the use of external light.

medium. This results in the emission of light. For medicinal applications, radioisotopes that are used for radiotherapy or PET imaging can be employed for the *in vivo* generation of CR. To date, the *in situ* excitation of a PDT agent with CL and CR has been demonstrated by Guo *et al.* with the synthesis of self-assembling, radioiodinated nanoparticles.[27] Within the acidic microenvironment of cancer cells, the nanoparticles disaggregate to produce the activated PDT agents. Another example is the co-delivery of titanocene (as PS) formulated in nanomicelles combined with [^{18}F]-fluorodeoxyglucose by Kotagiri *et al.*[28] Challenges associated with CR mediated, depth-independent phototherapy that arise from low photon production require combination of CR with ultra-high potency PDT agents or increase of delivered activity approaching limits set forth by clinical dosimetry.

Conclusively, *in situ* excitation strategies are well suited to enable the systemic application of PDT beyond localized, non-metastatic tumors. CL and BL appear as suitable strategies for *in situ*, co-delivery of photoexcitation sources. A severe drawback of both systems is the reliance on hydrogen peroxide or similar oxidative species. Tumor tissue is often hypoxic and therefore not optimal for such systems (*vide supra*).

3.5.3 Circumventing the scarcity and inherent toxicity of second and third row transition metals. A large part of the work on metal-based PDT agents focuses on second and third row transition metals due to their versatile chemical and photophysical properties. However, second and third row transition metals can be scarce when compared to first row transition metals, which may ultimately limit wide-ranging patient access to these therapies. Second, heavy metals possess inherent toxicity due to their ability to displace endogenous, first row transition metal ions within vital metalloenzymes, resulting in off target toxicity, best known as heavy metal poisoning.

A potential mitigation strategy is to employ first row transition metals for the design of new PDT agents by stabilizing complexes sufficiently to prevent rapid dissociation kinetics.

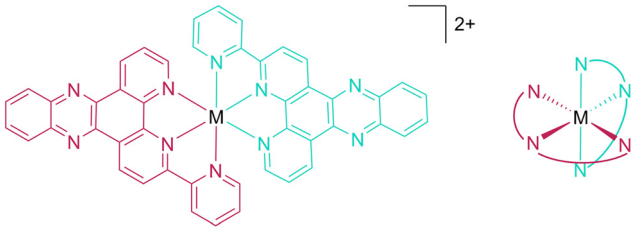

33 M = Fe
34 M = Ru

Fig. 14 Structures of **33** and **34**.

A recent review covers first row transition metal-based PDT agents.[29] First row transition metals are more abundant and better regulated by homeostasis when occurring at elevated concentrations *in vivo*. One example of this emerging compound class of PDT agents is complex **33**, an iron analogue of the Ru compound **34** (Fig. 14). It exhibits phototoxicity of 13.1 μM (MCF-7 cell line) and no cytotoxicity at concentrations of up to 100 μM in the dark. The 3-(pyridin-2-yl)dipyrido[3,2-*a*:2′,3′-*c*]phenazine (pydppz) ligand serves as a DNA intercalator. Under green light (556 nm) irradiation and in the presence of oxygen, DNA cleavage is observed.[29,30]

3.6 Emerging areas of interest

Photodynamic therapy with coordination complexes has extensive clinical potential for the treatment of various diseases due to its ability to closely control the temporal and spatial activity of a drug, thereby severely limiting off-target toxicity. However, PDT is subject to various limitations. The hypoxic nature of tumors limits the efficacy of PSs to produce ROS, the limited tissue penetration of light impedes the treatment of deep tumors or metastases, and the use of second and third row transition metals raises questions about resource availability, the price of potential pharmaceuticals and inherent heavy metal toxicity. The future of metal-based PDT agents requires strategies to overcome these issues.

A wide variety of strategies exist to address and overcome these challenges, yet they all rely on concomitant finetuning of the PS properties to suit the requirements of the employed system. Transition metal complexes are uniquely suited for this purpose, as their physicochemical properties can readily be changed by manipulation of their coordination sphere. Therefore, transition metal complexes will continue to play an important role in the development of the next generation of PDT agents.

4. Coordination complexes as enzyme active site inhibitors

4.1 Introduction

The majority of clinically utilized drugs are organic small molecules that act by reversible or irreversible inhibition of enzyme active or allosteric sites, thereby effectively inhibiting the target enzyme's function temporarily or permanently. The use of main group elements imposes geometric and reactivity constraints. A logical expansion beyond such constraints is to include coordination complexes. Coordination complexes exhibit unique features that make them ideal scaffolds for enzyme inhibitor design. Variation of coordination number, geometry and redox states gives rise to unique 3D geometries which can selectively target the enzymes of interest.[31] As a consequence, the inhibitory activity can be tuned by the modification of the coordination properties of the metal ion, its oxidation state and ligand structure.

Furthermore, at least one third of enzymes contain a metal ion within their active site to promote metabolic or catabolic processes. Dysregulation of metalloenzymes such as matrix metalloproteases (MMP), histone deacetylases (HDCA) or carbonic anhydrases (CA) can efficiently modulate the survival or growth progression of cancer cells.[32] Therefore, these metalloenzymes represent an attractive therapeutic target in cancer treatment by targeted modification of the coordination environment of the metal center within the enzyme's active site.

To target enzyme inhibition, coordination chemistry can be utilized following three distinct strategies: inert metal complexes as active-site binders (herein referred to as type I), metal complexes that displace endogenous metal centers in active sites (type II-A) and ligands that coordinate to enzyme active sites containing metal centers to block substrate access (type II-B) (Fig. 15).

4.2 Targeted enzyme inhibition with coordination complexes

4.2.1 Type I metal-based inhibitors: metal complexes as active-site binders. This first category refers to metal complexes

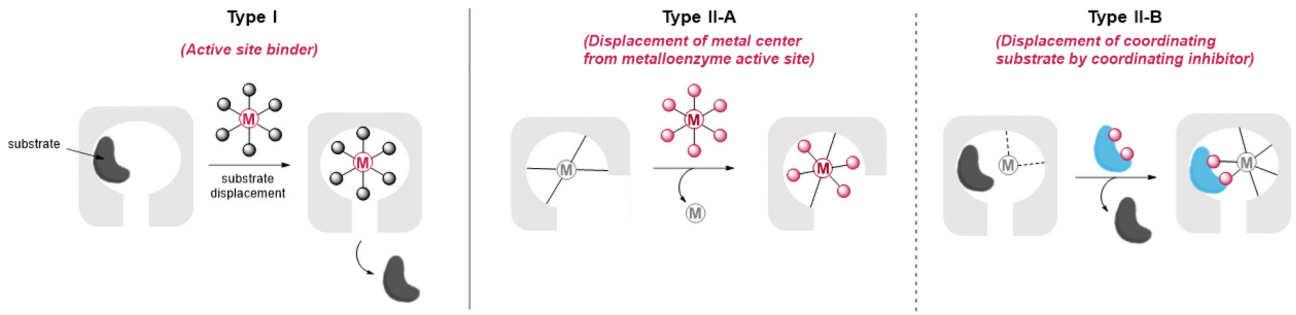

Fig. 15 Metal-based enzyme active site inhibitors and their mechanisms of action.

as active site binders. Rhenium tricarbonyl complexes have garnered particular interest as enzyme inhibitors due to their exceptional kinetic inertness and close control of electro- and photochemical reactivity governed by variation of ligand binding sites.

Human carbonic anhydrase inhibitors (hCAIs) comprised of organometallic Re^{+} complexes have been reported by Alberto *et al.* The reaction between CO_2 and water to produce carbonic acid is catalyzed by the zinc-dependent enzyme carbonic anhydrase. This represents an attractive target in cancer therapy due to its overexpression induced by hypoxia. Sulfonamide or sulfamate functional groups have been widely investigated to bind carbonic anhydrase. Rhenium complex **35** employs a cyclopentadienyl ligand that binds to the binding pocket of hCA with hydrophobic interactions with three amino acids Phe131, Leu198, and Pro202 (Fig. 16, left).[33]

Coumarin–Re conjugates constitute another class of CA inhibitors. Similarly, rhenium complex **36** is based on a bidentate pyridine–triazole ligand functionalized by a coumarin moiety (Fig. 16, middle). The triazole acts as a linker between the pharmacophore coumarin and the coordinating group pyridine. The mechanism of action of complex **36** involves the blocking of the enzyme cavity, producing the closed (non-hydrolyzed) and hydrolyzed form interaction of the *fac*-$Re(CO)_3$ moiety to efficiently encumber the active site.[34]

Most recently, Re^{+}–tricarbonyl compounds incorporating the 2,2′-bipyridine ligand have been described for the inhibition of cysteine protease to disrupt the viral life cycle of SARS-CoV-2.[35] The mechanism of action involves formation of a reversible covalent bond between the rhenium complex and the catalytically active cysteine amino acid in the active site. The Re^{+} complex **37** for which a water ligand was replaced by the thiol group of Cys135 demonstrated the highest inhibitory effect, likely due to electrostatic interactions of the amine substituents with the negatively charged surface (in red) within the binding pocket (Fig. 16, right).

Another example of type I inhibitors are V^{5+} oxo-species that efficiently mimic a transition state analog of phosphate. Because of the structural similarity to phosphate, these complexes are well suited for the selective inhibition of phosphatases (Fig. 17). For instance, orthovanadate (**38**) adopts a trigonal pyramidal geometry inside of the phosphatase active site. The coordination polyhedron is mostly stabilized by hydrogen bonds. V^{5+} complexes can mimic the effects of insulin by inhibition of the insulin receptor protein tyrosine phosphatase (PTPase). As first-generation vanadium salts resulted in gastrointestinal distress as principal sign of vanadium toxicity, inorganic vanadium compounds BMOV (**39**) and its ethylmaltol analog BEOV (**40**) were developed. BEOV successfully reached phase II clinical trials and demonstrated the reduction in fasting blood glucose.[36] As vanadium complexes display attractive properties for the treatment of diabetes and cancer, prospective ligand and complex design approaches must pursue systematic reduction of toxicity.

4.2.2 Type II-A metal-based inhibitors: displacement of endogenous metal ions from enzyme active sites. Metal complexes can also act as coordinative inhibitors by displacing endogenous metal ions in biological chelating agents such as proteins. For instance, octahedral Co^{3+}-sb complexes have been described by Meade *et al.* as effective zinc-finger inhibitors that irreversibly bind and inhibit the mechanism of action of zinc finger proteins (Fig. 18).[37] The mechanism of action, established using molecular dynamic simulations, involves displacement of endogenous Zn^{2+} with a Co^{2+} complex to irreversibly occupy the binding site of the protein. The inhibitory action of the Co^{3+} complex arises from changes to the secondary structure of the zinc finger protein induced by displacement of tetrahedral Zn^{2+} by octahedral the Co^{3+} complex.

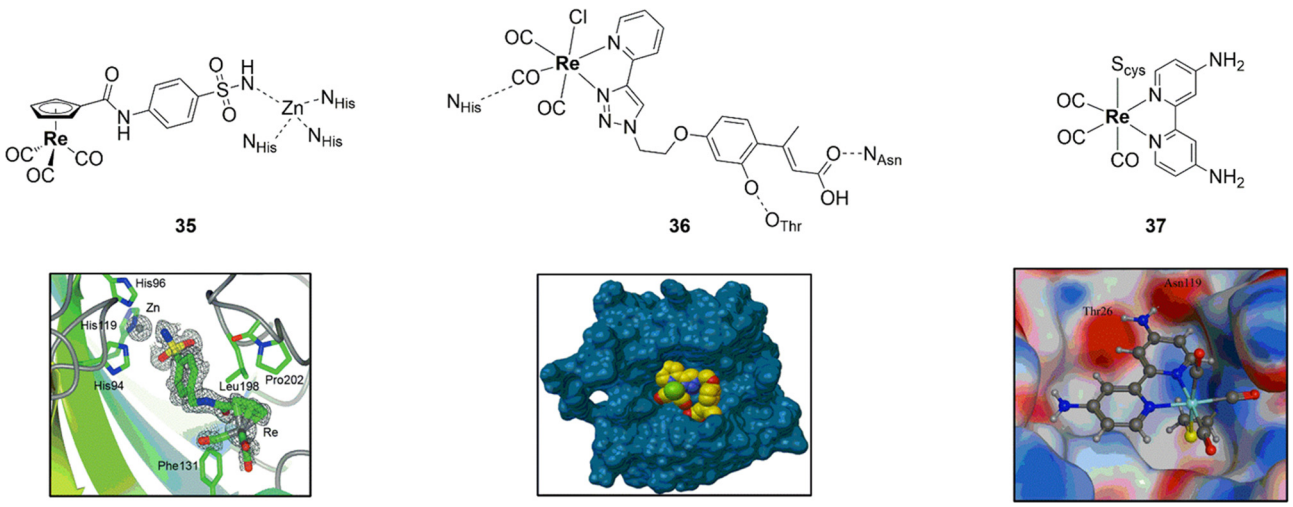

Fig. 16 Left: Structure of a cyclopentadienyl-based Re^{+} complex in the binding pocket of hCA II enzyme and the crystal structure of the major conformation. Figure from R. Alberto *et al.*, *Angew. Chem., Int. Ed.*, Wiley Online Library, 2012, **51**, 3354. Middle: Structure of a coumarin–Re^{+} conjugate and a representation of the shape complementarity with the binding pocket of hCA IX. Figure from A. Seridi *et al.*, *Crystals*, MDPI, 2021, **11**, 1076. Right: Structure of a bipyridine-based Re^{+} complex and the modelled binding pose targeting SARS-CoV2. Figure reproduced from S. M. Cohen, *et al.*, *Angew. Chem., Int. Ed.*, Wiley Online Library, 2021, **60**, 2.

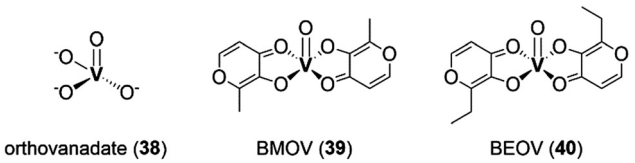

Fig. 17 Structure of vanadium complexes as phosphatases and insulin mimics.

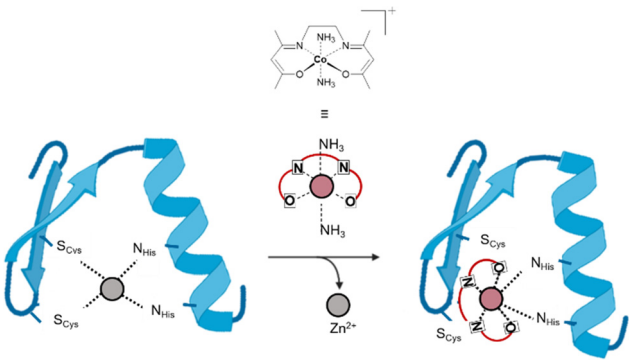

Fig. 18 Displacement of Zn^{2+} by Schiff-based Co^{3+} complex in zinc finger protein.

4.2.3 Type II-B metal-based inhibitors: coordinative modification of metal-containing active sites. Type II-B inhibitors act by blocking access of the substrate to the catalytic site by directly binding to the metal center within the active site of the enzyme.

Rpn11 and LpxC are two examples of Zn^{2+}-dependent enzymes whose inhibitions have emerged as a powerful strategy in anticancer therapy.[38] Their inhibitors contain a metal binding group and an organic backbone built to interact with the enzyme surface through non-covalent, hydrogen bonding, hydrophobic and electrostatic interactions (Fig. 20). The ubiquitin-proteasome system (UPS) plays an important role in metabolism and its inhibition has emerged as a powerful strategy in anticancer therapy. An 8-quinoline derivative with low micromolar IC_{50} values for Rpn11 was identified as the only hit from a small library screen. Through fragment growth design, the first-in-class Rpn11 inhibitor, capzimin (340 nM) in Fig. 19 was developed. The mechanism of inhibition arises from coordination of the catalytic Zn^{2+} center by Rpn11 in a bidentate manner through the endocyclic nitrogen and exocyclic sulfur donor atoms resulting in blocking of protein degradation by the proteasome.[39]

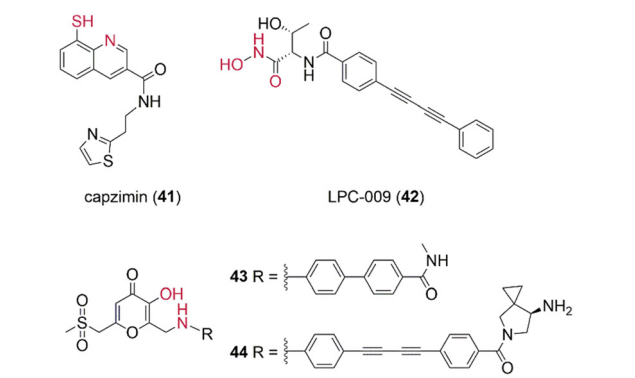

Fig. 19 Examples of Rpn11 and LpxC inhibitors.

LpxC is an emerging target to combat multidrug-resistance in Gram negative bacteria. The LpxC enzyme catalyzes the deacetylation through a Zn^{2+} active site and binding of the substrate through a hydrophobic tunnel. Fig. 20 (left panel) depicts the *E. coli* LpxC bound to reaction product uracil diphosphate (UDP)-3-*O*-[(3*R*)-3-hydroxymyristoyl]-alpha-D-glucosamine (myr-UDP-GlcN) and a phosphate ion from the crystallization buffer. The Zn^{2+} ion in the active site is four-fold coordinated in a tetrahedral geometry with two histidine and one aspartate residues, and the phosphate ion. Inhibitors such as LPC-009 (**32**) with linear diphenyl-acetylene moiety have been studied to facilitate the passage through the hydrophobic tunnel.

The crystal structure of **LPC-009** in the active site of *Pseudomonas aeruginosa* LpxC reveals the bidentate interaction of the hydroxamate moiety (Fig. 20, right). While originally promising, development of non-hydroxamate containing inhibitors of LpxC has become a priority since the hydroxamate-containing inhibitors were associated with side effects and failed in clinical trials. A series of novel non-hydroxamate LpxC inhibitors incorporating the hydroxypyrone moiety for Zn^{2+} coordination shows considerable promise in first pass preclinical experiments (**43** and **44** in Fig. 19).

4.3 Current challenges and opportunities

4.3.1 Limited chemical space. One challenge in the development of metal-based inhibitors is the limited number of metal-binding pharmacophores currently available to design inert systems with little chemical reactivity and high structural fidelity. Even though high-throughput screening (HTS) can produce compounds with high affinity, the lack of currently available, metal-containing structural isosteres still exhibits low coverage of the possibly vast, underexplored chemical space.

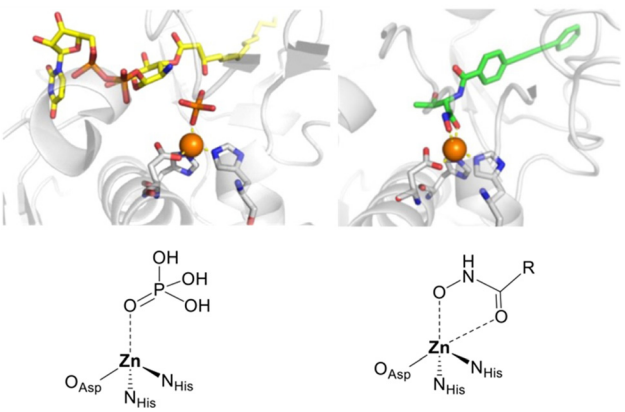

Fig. 20 Left: Interaction of myr-UDP-GlcN and phosphate ion in *E. coli* LpxC binding pocket (PDB 4MDT). Right: Interaction of LPC-009 inhibitor in *P. aeruginosa* LpxC binding pocket (PDB 3P3E). Figures reproduced with permission from {S. M. Cohen *et al.*, *Chem. Rev.*, 2019, **119**(2), 1323} Copyright {2019} American Chemical Society.

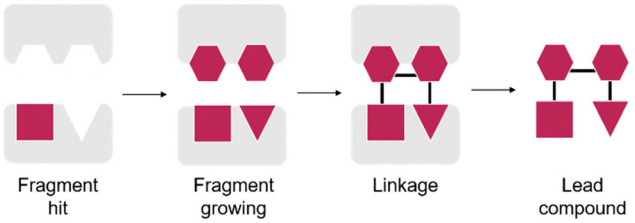

Fig. 21 Schematic description of the fragment-based drug design approach (FBDD).

To overcome this limitation, the screening of small fragment libraries has been proposed. Fragment-based drug design (FBDD) is now one of the main strategies in modern drug discovery. This approach is based on optimal filling of the available chemical space within the target site using libraries of small and diverse chemical fragments to inform the design of a corresponding single molecule inhibitor.[40] Combination of conventional, small molecule FBDD under inclusion of metal-binding pharmacophores can therefore enable discovery of metal-containing drug candidates with high binding affinities to the target of interest. An example for successful FBDD to develop a type II, metalloenzyme targeting small molecule inhibitor has already been documented and can be expanded upon with other metal-containing isosteres (Fig. 21).[41,42]

4.3.2 Need for improved computational methods. Computational strategies aim to model the operation mode of the transition metal complexes under biological conditions; however, these strategies lag far behind approaches already developed for organic structural fragments. The main reason for this discrepancy is the lack of computational techniques that can reliably model coordination complexes with nontrivial electronic structure. Therefore, the accurate prediction of binding affinities, geometries and interactions between the enzyme and metal-based inhibitors remains challenging.[43]

Over the years, density functional theory (DFT) calculations have become a powerful tool to predict molecular properties (geometries, thermodynamics, spectroscopic data) of transition metal complexes; however, DFT calculations remain time consuming and too complex to predict specific interactions of a transition metal complex with complex biomolecules. Molecular docking simulations have been widely used in medicinal chemistry, yet they remain inefficient to describe the formation/breaking bonds of the metal complexes and cannot describe the changes to the electronic structure of coordination complexes occurring during the binding process. Molecular dynamics requires more advanced computational methods to simulate these interactions, providing an opportunity for the development of force field simulations with diminished computational effort.[44] Hence, improved methods that can better approximate metal complex structures without the heavy computational burden of DFT and apply them subsequently in docking simulations outline a clear, to date unmet need.

4.3.3 Addressing target specificity and stability. Due to their pre-organized 3D scaffold, metal complexes can provide opportunities to enhance target specificity by complementing the enzyme binding site in shape and functional group presentation in ways inaccessible with organic small molecule fragments.[45]

Metal-based inhibitors take advantage of redox activity of metal ions. For instance, platinum complexes have been extensively explored using redox-mediated pro-drug activation strategies. Other complexes of first row transition metals Co, Fe and Cu can be stabilized in multiple oxidation states providing opportunities to selectively activate drugs at the target site by reducing or hypoxic microenvironments. The transition metal provides an inert framework for transportation of the inhibitor. Once exposed to a hypoxic environment, reduction of the coordination complex occurs, and the active inhibitor is released. For instance, Co^{3+} complexes have been used as prodrugs for enzyme inhibitors such as marimastat, a broad-spectrum matrix metalloproteinase inhibitor. Co^{3+} complexes are efficiently reduced in reducing tumor microenvironments to produce labile Co^{2+} complexes that readily release the drug cargo.[46]

Implementation of metal complex prodrug strategies requires careful consideration of ligand donor effects, substitution rates and redox potentials. Ideally, the inert prodrug–metal complex exhibits high stability in healthy tissues and the efficient release of the bioactive ligand under reductive environment. Another way to limit off-target toxicity is to attach a targeting ligand to the redox-active prodrug, enhancing the therapeutic effect and decreasing unwanted activation. For instance, several HDAC inhibitors have been coordinated to Pt^{4+} to form octahedral prodrugs. The corresponding redox-activated Pt^{2+} species efficiently released the HDAC inhibitor and demonstrated multifunctional action (Fig. 22).[47]

4.3.4 Using intrinsic optical or radioactive properties of metal complexes to elucidate mechanisms of action. Metal complexes exhibit intrinsic properties that are helpful to elucidate their mechanism of action *in vitro* and *in vivo*; these features arise predominantly from presence of d-electrons and therefore remain unique for coordination complexes in contrast to organic small molecules.

Several rhenium complexes have been investigated as an alternative to platinum-based drugs. These complexes exhibit rich spectroscopic properties that can be exploited by fluorescent imaging, making them observable in cellular environments. Indeed, the triplet-based luminescent emission of many Re^{+}–tricarbonyl complexes allowed their study using fluorescence imaging applications. Furthermore, vibrational

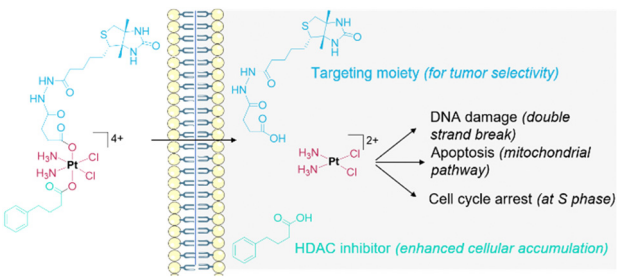

Fig. 22 Multifunctional Pt^{4+} complex as redox prodrug.

microscopy can be performed to detect the characteristic, distinct CO stretching frequency of the $Re^{+}(CO)_3$ core. In addition, the real-time tracking of these complexes in biological environments is possible due to their high photostability and lack of endogenous metal content background. Cellular uptake and distribution can be determined accurately by ICP-MS (Inductively Coupled Plasma-Mass Spectrometry) or Atomic Absorption Spectroscopy (AAS), yet these methods provide no information on speciation of the corresponding complex.

In contrast, observation of a characteristic, spectroscopic property can be indicative of the compound's speciation and intact nature. For instance, complex **45**, a polypyridine $Re^{+}(CO)_3$ complex bearing an isonitrile axial ligand, is luminescent upon irradiation with UVA and blue light and highly stable over a week. This complex was fully characterized by conventional spectroscopic tools and further employed for confocal fluorescent microscopy. The authors were able to identify complex **45** as an effective apoptotic agent by triggering ER stress and unfolded protein response pathway as visualized by microscopy studies. The stability of the axial ligand was also evaluated by X-Ray Fluorescence Microscopy (XFM) using complex **46** to compare the elemental distribution of the iodide of the axial ligand and Re in cells. Re and I elemental maps were coincided, indicating that the axial ligand remains bound to the metal center within the cell (Fig. 23).[48]

Isotope tracking is another convenient approach to elucidation of compound mechanism of action. Radiotracing to elucidate pharmacokinetics is becoming increasingly attractive to predict drug behavior in medicinal chemistry. An example of the application of a radiotagged analogue is the recent development of a siderophore-based antibiotic for the treatment of infection. Siderophores are naturally produced by pathogenic bacteria to scavenge iron from the host and increase survival and proliferation. Many synthetic siderophore–antibiotic conjugates have been developed and used iron uptake pathway to release the antibiotics in the cytoplasm of the bacteria.

Based on this and the chemical similarity between Fe^{3+} and Ga^{3+}, a Ga-desferrichrome siderophore conjugate linked to ciprofloxacin (galbofloxacin, **47**) has been developed. Compound

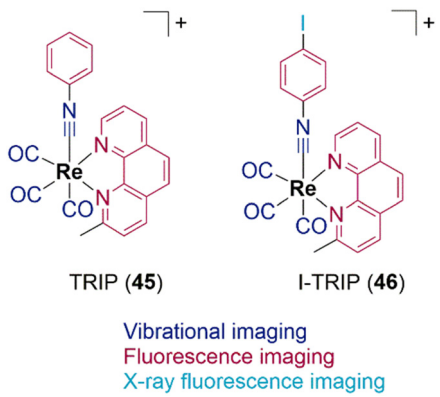

Fig. 23 Examples of Re^{+} complexes providing opportunities for spectroscopic study with vibrational and fluorescence imaging techniques.

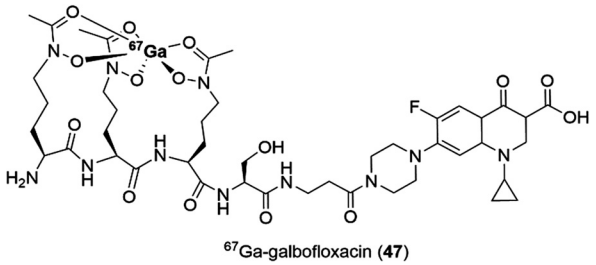

Fig. 24 ^{67}Ga-Desferrichrome siderophore conjugate linked ciprofloxacin (^{67}Ga-galbofloxacin) as an example for a metal-based drug molecule where radioactive tracing was employed to study pharmacokinetic behavior.

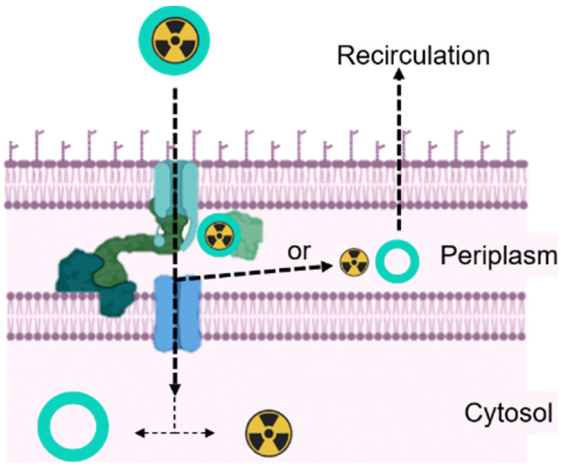

Fig. 25 Isotope tracking of siderophore-based conjugates to investigate active transport mediated uptake in bacteria.

47 demonstrated enhanced efficacy in treating Gram positive infections in a mouse model. The corresponding radiochemically tagged analogue ^{67}Ga-galbofloxacin (Fig. 24) uncovered critical information on the compound's ability to accumulate in infected tissues and provided general pharmacokinetic information (Fig. 25).[49]

4.4 Emerging areas of interest

The development of metal-based inhibitors represents a growing field of interest in research of therapeutic or diagnostic compounds. Due to their versatile properties, metal complexes remain a valuable scaffold to construct metalloenzyme inhibitors that can either structurally mimic the enzyme active site or interact with or displace the active metal ion. The investigation of their mechanism of action can further be conducted using their intrinsic spectroscopic properties as well as radiotracing, when feasible.

Primary challenges remain due to the relative novelty of this area of research, as metal-based compounds remain vastly understudied in comparison with organic small molecules used in medicinal chemistry. The greater the chemical space becomes that can be covered with known and novel metal complexes, the more enzyme active sites can become viable

targets. Furthermore, introduction of metal complexes for medicinal chemistry applications also bears the risk of unpredictable toxicity, especially as the biological behavior of many exogenous metal ions remains poorly understood.

5. Conclusions and outlook

While this tutorial review focused on three specific subtopics of Medicinal Inorganic Chemistry, it is important to emphasize that the covered material is in no way exhaustive nor fully representative of the rich and innovative approaches to diagnostic and therapeutic intervention provided by metal complexes. Metals and metalloids cover vast chemical space when compared to commonly explored main group elements in medicinal chemistry. As metal complexes also remain underexplored with respect to their photophysical, solution and electrochemical nature especially in aqueous and biologically relevant environments, work in this field bears extensive, thus far untapped potential.

Conflicts of interest

There are no conflicts to declare.

Acknowledgements

Jennifer Whetter and Minhua Cao are acknowledged for providing several figure drawings appearing in this review article and editing of the written text. E. B. acknowledges the National Institutes for General Medicine (NIGMS, R35GM142770), the National Institutes of Biomedical Imaging and Bioengineering (NIBIB, R21EB030071-01A1) and the Gordon and Betty Moore Foundation for funding.

References

1 T. I. Kostelnik and C. J. C. R. Orvig, *Chem. Rev.*, 2018, **119**, 902–956.
2 A. Duatti, *Nucl. Med. Biol.*, 2021, **92**, 202–216.
3 J. M. Kelly, A. Amor-Coarasa, E. Sweeney, J. J. Wilson, P. W. Causey and J. W. Babich, *EJNMMI Radiopharm. Chem.*, 2021, **6**, 1–14.
4 J. J. Woods, R. Unnerstall, A. Hasson, D. S. Abou, V. Radchenko, D. L. Thorek and J. J. Wilson, *Inorg. Chem.*, 2022, **61**, 3337–3350.
5 T. A. Bailey, V. Mocko, K. M. Shield, D. D. An, A. C. Akin, E. R. Birnbaum, M. Brugh, J. C. Cooley, J. W. Engle and M. E. Fassbender, *Nat. Chem.*, 2021, **13**, 284–289.
6 T. A. Bailey, J. N. Wacker, D. D. An, K. P. Carter, R. C. Davis, V. Mocko, J. Larrabee, K. M. Shield, M. N. Lam and C. H. Booth, *Nucl. Med. Biol.*, 2022, **110–111**, 28–36.
7 A. J. Koller, S. Saini, I. F. Chaple, M. A. Joaqui-Joaqui, B. M. Paterson, M. T. Ma, P. J. Blower, V. C. Pierre, J. R. Robinson, S. E. Lapi and E. Boros, *Angew. Chem., Int. Ed.*, 2022, e202201211, DOI: **10.1002/anie.202201211**.
8 I. F. Chaple, H. A. Houson, A. Koller, A. Pandey, E. Boros and S. E. Lapi, *Nucl. Med. Biol.*, 2022, **108–109**, 16–23.
9 B. A. Broder, M. P. Bhyuian, R. Freifelder, H. J. Zhang, A. Kucharski, M. W. Makinen, D. A. Rotsch and C.-T. Chen, *Appl. Radiat. Isot.*, 2022, **186**, 110270.
10 L. Ma, C. Grant, F. Gallazzi, L. D. Watkinson, T. L. Carmack, M. F. Embree, C. J. Smith, D. Medvedev, C. S. Cutler and Y. Li, *Nucl. Med. Biol.*, 2022, **108**, 61–69.
11 F. Najafi Khosroshahi, Y. Feng, L. Ma, S. Manring, T. L. Rold, F. A. Gallazzi, S. P. Kelley, M. F. Embree, H. M. Hennkens and T. J. Hoffman, *Bioconjugate Chem.*, 2021, **32**, 1364–1373.
12 A. Ingham, T. I. Kostelnik, B. L. McNeil, B. O. Patrick, N. Choudhary, M. de Guadalupe Jaraquemada-Peláez and C. Orvig, *Dalton Trans.*, 2021, **50**, 11579–11595.
13 B. L. McNeil, K. J. Kadassery, A. W. McDonagh, W. Zhou, P. Schaffer, J. J. Wilson and C. F. Ramogida, *Inorg. Chem.*, 2022, **61**, 9638–9649.
14 B. L. McNeil, A. K. Robertson, W. Fu, H. Yang, C. Hoehr, C. F. Ramogida and P. Schaffer, *EJNMMI Radiopharm. Chem.*, 2021, **6**, 1–18.
15 J. Fong, K. Kasimova, Y. Arenas, P. Kaspler, S. Lazic, A. Mandel and L. Lilge, *Photochem. Photobiol. Sci.*, 2015, **14**, 2014–2023.
16 P.-Y. Liao, X.-R. Wang, Y.-H. Gao, X.-H. Zhang, L.-J. Zhang, C.-H. Song, D.-P. Zhang, Y.-J. Yan and Z.-L. Chen, *Bioorg. Med. Chem.*, 2016, **24**, 6040–6047.
17 R. M. Khaled, A. Friedrich, M. A. Ragheb, N. T. Abdel-Ghani and A. M. Mansour, *Dalton Trans.*, 2020, **49**, 9294–9305.
18 C. Huang, C. Liang, T. Sadhukhan, S. Banerjee, Z. Fan, T. Li, Z. Zhu, P. Zhang, K. Raghavachari and H. Huang, *Angew. Chem., Int. Ed.*, 2021, **60**, 9474–9479.
19 R. Lincoln, L. Kohler, S. Monro, H. Yin, M. Stephenson, R. Zong, A. Chouai, C. Dorsey, R. Hennigar, R. P. Thummel and S. A. McFarland, *J. Am. Chem. Soc.*, 2013, **135**, 17161–17175.
20 S. Monro, K. L. Colón, H. Yin, J. Roque, P. Konda, S. Gujar, R. P. Thummel, L. Lilge, C. G. Cameron and S. A. McFarland, *Chem. Rev.*, 2019, **119**, 797–828.
21 V. Venkatesh and P. J. Sadler, in *Metallo-Drugs: Development and Action of Anticancer Agents*, ed. A. Sigel, H. Sigel, E. Freisinger and R. K. O. Sigel, Walter de Gruyter GmbH, Berlin, 2018, ch. 3, vol. 18, pp. 69–108.
22 B. Ferrari, E. Roda, E. C. Priori, F. De Luca, A. Facoetti, M. Ravera, F. Brandalise, C. A. Locatelli, P. Rossi and M. G. Bottone, *Front. Neurosci.*, 2021, **15**, 589906.
23 W. Han, W. He, Y. Song, J. Zhao, Z. Song, Y. Shan, W. Hua and Y. Sun, *Dalton Trans.*, 2022, **51**, 7343–7351.
24 A. Zamora, C. A. Denning, D. K. Heidary, E. Wachter, L. A. Nease, J. Ruiz and E. C. Glazer, *Dalton Trans.*, 2017, **46**, 2165–2173.
25 L. Huang, S. Zhao, J. Wu, L. Yu, N. Singh, K. Yang, M. Lan, P. Wang and J. S. Kim, *Coord. Chem. Rev.*, 2021, **438**, 213888.
26 Y. Zhang, Y. Hao, S. Chen and M. Xu, *Front. Chem.*, 2020, **8**, 770.
27 J. Guo, K. Feng, W. Wu, Y. Ruan, H. Liu, X. Han, G. Shao and X. Sun, *Angew. Chem., Int. Ed.*, 2021, **60**, 21884–21889.

28 N. Kotagiri, M. L. Cooper, M. Rettig, C. Egbulefu, J. Prior, G. Cui, P. Karmakar, M. Zhou, X. Yang, G. Sudlow, L. Marsala, C. Chanswangphuwana, L. Lu, L. Habimana-Griffin, M. Shokeen, X. Xu, K. Weilbaecher, M. Tomasson, G. Lanza, J. F. DiPersio and S. Achilefu, *Nat. Commun.*, 2018, **9**, 275.
29 L. Gourdon, K. Cariou and G. Gasser, *Chem. Soc. Rev.*, 2022, **51**, 1167–1195.
30 A. Garai, U. Basu, I. L. A. Pant, P. Kondaiah and A. R. Chakravarty, *Chem. Sci.*, 2015, **127**, 609–618.
31 J. Karges, R. W. Stokes and S. M. Cohen, *Trends Chem.*, 2021, **3**, 523–534.
32 J. Iqbal, C. Jacob and J. Sévigny, *Front. Pharmacol.*, 2021, **12**, 746925.
33 D. Can, B. Spingler, P. Schmutz, F. Mendes, P. Raposinho, C. Fernandes, F. Carta, A. Innocenti, I. Santos and C. T. Supuran, *Angew. Chem., Int. Ed.*, 2012, **51**, 3354–3357.
34 Y. Aimene, R. Eychenne, F. Rodriguez, S. Mallet-Ladeira, N. Saffon-Merceron, J.-Y. Winum, A. Nocentini, C. T. Supuran, E. Benoist and A. Seridi, *Crystals*, 2021, **11**, 1076.
35 J. Karges, M. Kalaj, M. Gembicky and S. M. Cohen, *Angew. Chem.*, 2021, **133**, 10811–10818.
36 S. Treviño, A. Díaz, E. Sánchez-Lara, B. L. Sanchez-Gaytan, J. M. Perez-Aguilar and E. González-Vergara, *Biol. Trace Elem. Res.*, 2019, **188**, 68–98.
37 C. R. Brue, M. W. Dukes, M. Masotti, R. Holmgren and T. J. Meade, *ChemMedChem*, 2022, **17**, e202200025.
38 A. Y. Chen, R. N. Adamek, B. L. Dick, C. V. Credille, C. N. Morrison and S. M. Cohen, *Chem. Rev.*, 2018, **119**, 1323–1455.
39 C. Perez, J. Li, F. Parlati, M. Rouffet, Y. Ma, A. L. Mackinnon, T.-F. Chou, R. J. Deshaies and S. M. Cohen, *J. Med. Chem.*, 2017, **60**, 1343–1361.
40 C. N. Morrison, K. E. Prosser, R. W. Stokes, A. Cordes, N. Metzler-Nolte and S. M. Cohen, *Chem. Sci.*, 2020, **11**, 1216–1225.
41 B. L. Dick and S. M. Cohen, *Inorg. Chem.*, 2018, **57**, 9538–9543.
42 M. K. Jackl, H. Seo, J. Karges, M. Kalaj and S. M. Cohen, *Chem. Sci.*, 2022, **13**, 2128–2136.
43 I. Tolbatov and A. Marrone, *Inorg. Chim. Acta*, 2022, **530**, 120686.
44 G. Palermo, A. Spinello, A. Saha and A. Magistrato, *Exp. Opin. Drug Discovery*, 2021, **16**, 497–511.
45 E. Meggers, *Angew. Chem., Int. Ed.*, 2011, **50**, 2442–2448.
46 T. W. Failes, C. Cullinane, C. I. Diakos, N. Yamamoto, J. G. Lyons and T. W. Hambley, *Chem. – Eur. J.*, 2007, **13**, 2974–2982.
47 W. Han, W. He, Y. Song, J. Zhao, Z. Song, Y. Shan, W. Hua and Y. Sun, *Dalton Trans.*, 2022, **51**, 7343–7351.
48 C. C. Konkankit, J. Lovett, H. H. Harris and J. J. Wilson, *Chem. Commun.*, 2020, **56**, 6515–6518.
49 A. Pandey, C. Savino, S. H. Ahn, Z. Yang, S. G. Van Lanen and E. Boros, *J. Med. Chem.*, 2019, **62**, 9947–9960.